Available online at www.sciencedirect.com
SCIENCE DIRECT®
Biochemical and Biophysical Research Communications 330 (2005) 247–252
BBRC
www.elsevier.com/locate/ybbrc

Site-specific DNA cleavage by artificial zinc finger-type nuclease with cerium-binding peptide ☆,☆☆

Takako Nakatsukasa, Yasuhisa Shiraishi, Shigeru Negi, Miki Imanishi, Shiroh Futaki, Yukio Sugiura *

Institute for Chemical Research, Kyoto University, Uji, Kyoto 611-0011, Japan

Received 16 February 2005

Abstract

The addition of a new function to native proteins is one of the most attractive protein-based designs. In this study, we have converted a C_2H_2-type zinc finger as a DNA-binding motif into a novel zinc finger-type nuclease by connecting two distinct zinc finger proteins (Sp1 and GLI) with a functional linker possessing DNA cleavage activity. As a DNA cleavage domain, we chose an analogue of the metal-binding loop (12 amino acid residues), peptide P1, which has been reported to exhibit a strong binding affinity for a lanthanide ion and DNA cleavage ability in the presence of Ce(IV). Our newly designed nucleases, Sp1(P1)GLI and Sp1(P1G)GLI, can strongly bind to a lanthanide ion and show a unique DNA cleavage pattern, in which certain positions between the two DNA-binding sites are specifically cleaved. The present result provides useful information for expanding the design strategy for artificial nucleases.

Keywords: Zinc finger protein; Lanthanide ion; Calcium-binding loop; DNA binding; DNA cleavage; Artificial nuclease

The complete analysis of the human genome reveals close relationships between DNA sequences and diseases. Therefore, the application of this knowledge to gene therapy has become of great importance. In order to desire high selectivity for a target DNA sequence, the construction of an artificial nuclease has been investigated widely as a promising tool [1–12]. One of the most versatile strategies is the concept that a metal-chelating ligand or a catalytic domain of a restriction enzyme is connected to DNA-binding proteins [1–10] or motifs [11,12]. In these approaches, the catalytic domains have been designed to locate at one side of the DNA-binding domain, and thus the DNA cleavage site was observed in the vicinity of the DNA-binding site, together with fluctuation in the DNA cleavage. To achieve a highly site-specific DNA cleavage inside the DNA recognition site, we first designed novel nucleases in which the catalytic domain is held by two DNA-binding domains.

A C_2H_2-type zinc finger motif is one of the most promising molecules for a DNA-binding domain of a nuclease for the following reasons [13–15]: (i) artificial zinc finger motifs for any DNA sequences are easily designed, because each domain strongly recognizes three-base-pairs with amino acid residues at specific positions in the α-helix, and (ii) this motif has a tandemly connected structure with the linker region. In our opinion,

☆ This study was supported in part by Grants-in-Aid for COE Project "Element Science" (12CE2005) and Scientific Research (16659028 · 14370755) from the Ministry of Education, Culture, Sports, Science and Technology, Japan. Y. Shiraishi is a Research Fellow of the Japan Society for the Promotion of Science.
☆☆ *Abbreviations:* Tris, tris(hydroxymethyl)aminomethane; TN, Tris–NaCl; CD, circular dichroism; zf, zinc finger; NMR, nuclear magnetic resonance.
* Corresponding author. Fax: +81 774 32 3038.
E-mail address: sugiura@scl.kyoto-u.ac.jp (Y. Sugiura).

0006-291X/$ - see front matter © 2005 Elsevier Inc. All rights reserved.
doi:10.1016/j.bbrc.2005.02.164

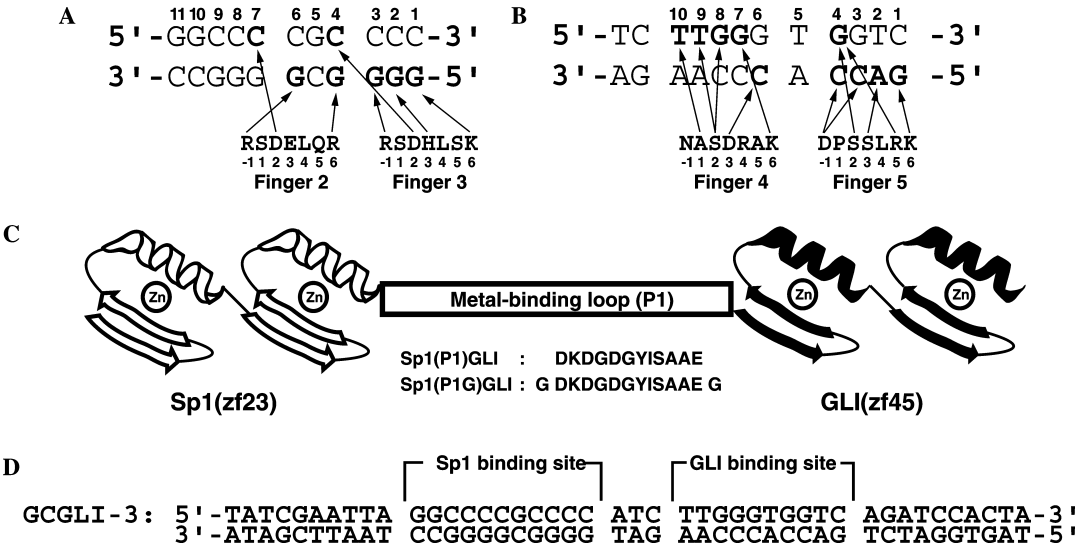

Fig. 1. (A,B) Base recognition mode of Sp1(zf23) and GLI(zf45) determined from NMR or X-ray analysis. Amino acid residues at the N-terminus of the α-helix in each finger are depicted by their one-letter codes with the number of helical positions below. Solid arrows show the base recognition, and the bases recognized by amino acids are written in bold characters. (C) Schematic representation of designed zinc finger-type nucleases. The designation of each zinc finger is shown by the original name. The amino acid residues of each peptide are indicated by their one-letter codes. (D) Substrate DNAs used in this study.

the conversion of the linker region into a functional linker with DNA cleavage ability should result in site-specific DNA cleavage. Considering steric hindrance, a short peptide is suitable for the DNA cleavage domain. The analogue (P1) of a 12-residue calcium-binding loop (sequence: DKDGDGYISAAE) strongly and specifically binds to a lanthanide ion [16–19]. On the other hand, chimeric molecules composed of DNA-binding domains and a Ce(IV)-based catalytic domain have been designed, because Ce(IV)-chelates have been reported to catalyze DNA hydrolysis with high efficiency [7–12]. In this research, we inserted the P1-Ce(IV) complex as a linker to connect two different zinc finger motifs. We previously reported that a peptide segment corresponding to fingers 2 and 3 of the Sp1 zinc finger (Sp1(zf23)) or to fingers 4 and 5 of the GLI zinc finger (GLI(zf45)) has sufficient DNA-binding affinity for their binding sites (Figs. 1A and B) [20–23]. In this report, based on these findings, we newly created the unique zinc finger-type nucleases, Sp1(P1)GLI and Sp1(P1G)GLI (Fig. 1C). In Sp1(P1)GLI, P1 was placed between Sp1(zf23) and GLI(zf45). In Sp1(P1G)GLI, glycine residues were inserted at both ends of peptide P1 of Sp1(P1)GLI to achieve subtle flexibility. This study describes the characteristics of their unique DNA cleavage properties and the potential of our approach in designing sophisticated metallonucleases.

Materials and methods

Chemicals. Fmoc-amino acid derivatives and peptide resin were purchased from Novabiochem and Applied Biosystems. The T4 polynucleotide kinase and restriction enzymes were obtained from New England Biolabs. The *Taq* DNA polymerase and synthesized oligonucleotides for cloning each peptide were acquired from Qiagen and Sigma Genosys, respectively. The labeled [γ-^{32}P]ATP compound was supplied by DuPont. The plasmid pBS-Sp1-fl was kindly provided by Dr. R. Tjian. All other chemicals were of commercial reagent grade.

Peptide synthesis. The peptide P1 (DKDGDGYISAAE-amide) was prepared by Fmoc-solid-phase synthesis on a TGS-RAM resin (Shimadzu). The peptide chain was constructed using a Shimadzu PSSM-8 synthesizer with a standard protocol including a benzotriazole-1-yl-oxy-tris-pyrrolidino-phosphonium hexafluorophosphate (PyBOP)/1-hydroxybenzotriazole (HOBt)/4-methylmorpholine (NMM) coupling system. The peptide segment was removed from the resin and deprotected by a treatment with trifluoroacetic acid/1,2-ethanedithiol (95:5) at room temperature for 2 h, followed by HPLC-purification on a Cosmosil 5C_{18}-ARII (10 mm × 250 mm) column (Nakalai Tesque). The fidelity of the product was confirmed by matrix-associated laser desorption ionization time-of-flight mass spectrometry (MALDI-TOF-MS) using a Voyager-DE STR system (Applied Biosystems): P1 [$M + H^+$] calcd. 1240.3, observed 1240.2.

Construction of zinc finger-type nucleases and substrate DNA fragments. Sp1(zf23) and GLI(zf45) are coded on the plasmids pEVSp1(566–623) and pEVGLI(99–160), respectively, as previously described [21,22]. The fragments of Sp1(zf23) and GLI(zf45) were amplified and combined with the fragment coded P1 sequence using the standard PCR technique. The resultant fragments were digested by restriction enzymes (*Nde*I and *Eco*RI) and inserted into pEV3b. Their sequences were confirmed by a GeneRapid DNA sequencer (Amersham Biosciences). These peptides were overexpressed as a soluble form in the *Escherichia coli* strain BL21(DE3)pLysS at 20 °C and purified according to the following procedure at 4 °C. *E. coli* cells were resuspended and lysed in PBS buffer. After centrifugation, the supernatant containing the soluble form of the zinc finger peptides was purified by cation-exchange chromatography using a 0.05–2.0 M NaCl gradient (Mono S HR 5/5; Amersham Biosciences). Final purification was achieved by a gel filtration technique (Superdex 75; Amersham Biosciences) using TN buffer [10 mM Tris–HCl (pH 8.0), 50 mM NaCl, and 1 mM dithiothreitol]. To prepare the substrate DNA, oligonucleotides containing the DNA-binding sites of Sp1(zf23) and

GLI(zf45) were provided (Fig. 1D); (GCGLI-3G: 5′-TAGTGG ATCTGACCACCCAAGATGGGGCGGGGCCTAATTCGATA-3′, and GCGLI-3C: 5′-TATCGAATTAGGCCCCGCCCCATCTTGG GTGGTCAGATCCACTA-3′). GCGLI-3G was labeled at the 5′-end with ^{32}P using a T4 polynucleotide kinase. After removing the unincorporated [γ-^{32}P]ATP with a G-50 Probe Quant (Amersham Biosciences), it was annealed with GCGLI-3C.

CD measurements. The CD spectra for all the peptides were recorded on a Jasco J-720 spectropolarimeter using a 0.10-cm path length quartz cell at 20 °C. The CD spectra are averages of 10 scans, collected at 0.5 nm intervals between 200 and 280 nm. All the CD samples were diluted to obtain 50 μM of the peptide P1 and 10 μM of zinc finger proteins in 10 mM Tris–HCl (pH 8.0), 50 mM NaCl, and 1 mM dithiothreitol.

Fluorescence determinations. Tb^{3+} luminescence sensitized by the Tyr residue in P1 was used for detecting the lanthanide ion-binding ability. Fluorescence emission spectra were conducted on a Shimadzu RF-5300PC using a 5.5-mm path length quartz cell. Aliquots (1 μl) of a concentrated stock solution of $TbCl_3$ in H_2O were added to each peptide over a range of Tb^{3+} concentrations from 0 to 40 μM. All experiments were conducted at 20 °C in 10 mM Tris–HCl (pH 8.0), 50 mM NaCl, and 1 mM dithiothreitol. After excitation of the sample at 280 nm, Tb^{3+} emission was recorded at 542 nm.

The data were fit to the following equation [24] using the Kaleida Graph program (Abelbeck software):

$$I = I_{max}[Tb^{3+}]_F/([Tb^{3+}]_F + K_{Tb^{3+}}),$$

where I is the Tb^{3+} emission at a particular Tb^{3+} concentration, I_{max} corresponds to the Tb^{3+} emission when the system is saturated, $[Tb^{3+}]_F$ is the free or nonbound Tb^{3+} concentration after each addition, and $K_{Tb^{3+}}$ is the equilibrium dissociation constant. $[Tb^{3+}]_F$ was determined: $[Tb^{3+}]_F = [Tb^{3+}]_T - [Tb^{3+}]_B$, where $[Tb^{3+}]_T$ and $[Tb^{3+}]_B$ correspond to the total and bound Tb^{3+} concentrations, respectively. Based on the assumption that I_{max} corresponds to 100% protein saturation (30 μM), $[Tb^{3+}]_B$ was calculated from $[Tb^{3+}]_B = (I)(30/I_{max})$.

Gel mobility shift assays. Gel mobility shift assays were carried out under the following conditions. Each reaction mixture contained 10 mM Tris–HCl (pH 8.0), 50 mM NaCl, 1 mM dithiothreitol, 20 μg/μl sonicated calf thymus DNA, 0.05% Nonidet P-40, 5% glycerol, 40 μg/ml bovine serum albumin, the ^{32}P-end-labeled substrate DNA fragment (~50 pM, 500 cpm), and 0–2 μM of the zinc finger protein. After incubation at 20 °C for 30 min, the sample was run on an 8% polyacrylamide gel with 89 mM Tris–borate buffer at 20 °C. The bands were visualized by autoradiography and quantified with ImageMaster 1D Elite software (version 3.01). The dissociation constants (K_d) of protein–DNA fragment complexes were estimated according to a previously reported procedure [21].

DNA cleavage analyses. Maxam–Gilbert sequencing reaction specimens were prepared as size and sequence markers by standard protocols. Various concentrations of peptides and 5 μM $(NH_4)Ce(NO_3)_6$ were incubated with the sample containing 10 mM Tris–HCl (pH 8.0), 50 mM NaCl, 1 mM dithiothreitol, 20 μg/μl sonicated calf thymus DNA, and the ^{32}P-end-labeled substrate DNA fragment (~8 nM, 40 Kcpm) at 37 °C. The reaction was stopped by adding an equivolume of phenol/chloroform. After ethanol precipitation, the cleaved products were analyzed on a 15% polyacrylamide/7 M urea sequencing gel. The bands were visualized by autoradiography.

Results and discussion

CD spectral features of peptides

The CD spectra of peptides at 20 °C are presented in Fig. 2. The spectrum around 214 nm is changed by the addition of La^{3+} to P1, and this result indicates that, under our buffer condition, P1 induced a structural change in response to La^{3+} the same as in the previous result under another buffer condition [19]. Furthermore, we examined the CD spectra of Sp1(P1)GLI and Sp1(P1G)GLI to confirm the fact that La^{3+} does not have a crucial effect on the structure of zinc finger peptides. Fig. 2B presents the CD spectra of Sp1(P1)GLI. The characteristic CD pattern of zinc finger peptides, which shows negative Cotton effects in the far-UV region with a minimum around 208 nm and a shoulder around 222 nm [22], is conserved in the presence of excess La^{3+}.

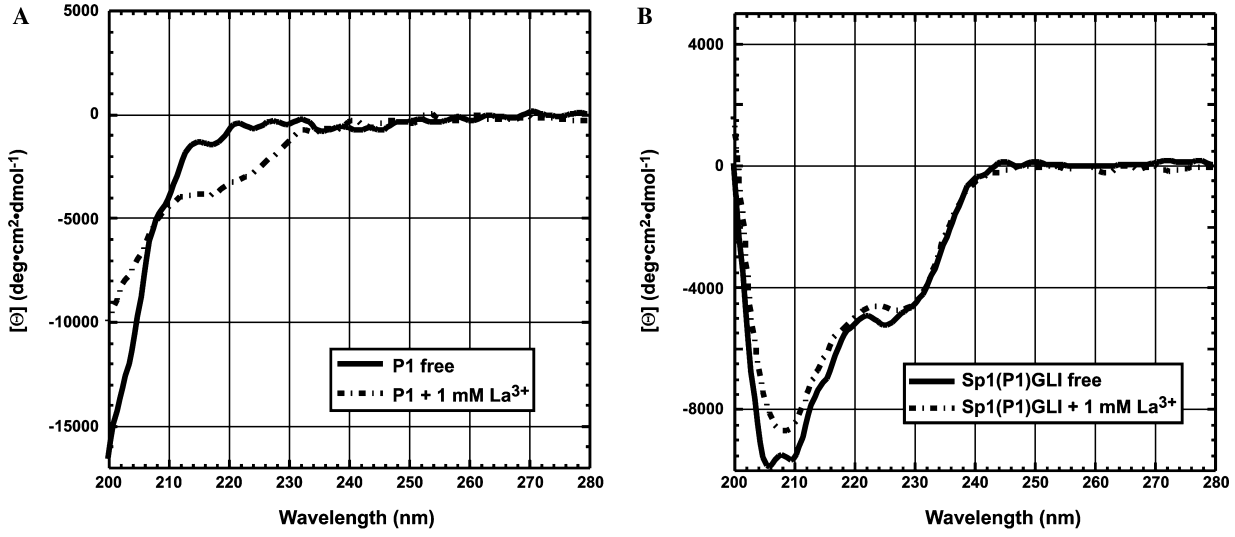

Fig. 2. CD spectra of P1 and Sp1(P1)GLI at 20 °C, respectively (A,B). In each panel, the peptides in free state or with 1 mM La^{3+} addition are indicated by the solid line and dashed line, respectively.

Detection of lanthanide ion-binding by terbium luminescence

When terbium (Tb^{3+}) is added to a solution including a lanthanide ion-binding peptide, strong terbium luminescence at 542 nm is observed [24,25]. The plots of the peptide fraction saturated with Tb^{3+} (I/I_{max}) versus Tb^{3+} concentration are shown in Fig. 3. The designed proteins, Sp1(P1)GLI and Sp1(P1G)GLI, exhibited an increase in luminescence at 542 nm according to the Tb^{3+} concentration in the same manner as reported for P1 [16]. Furthermore, fitting with the binding isotherms yielded the dissociation constants of both proteins ($K_{Tb^{3+}} = 5.4$ and 9.1 μM, respectively), which are in good agreement with the previous $K_{Tb^{3+}}$ values of lanthanide ion-binding peptides [8,25]. These results demonstrate that the P1 region in both proteins effectively binds to a lanthanide ion without steric disturbance by the zinc finger domains. Additionally, the equivalent binding of both proteins to Tb^{3+} reveals that the glycine spacers play no significant role in binding to a lanthanide ion.

DNA-binding affinity of each zinc finger protein

In a preliminary experiment, we found that GA was needed at the 5′ site of the GLI(zf45)-binding site for optimal binding of GLI(zf45). Therefore, we designed substrate GCGLI-3 by inserting GAT between two DNA-binding sites (Fig. 1D). Based on the gel mobility shift assays, the DNA-binding affinity (K_d) of designed proteins was determined for GCGLI-3 (Table 1). Sp1(P1)GLI and Sp1(P1G)GLI exhibited a similar DNA-binding affinity for GCGLI-3 ($K_d = 260$ and 280 nM, respectively), suggesting that the glycine spacers have no significant effect on DNA-binding affinity. Based on the previous results in which P1 formed a rigid structure and dimerized by binding to a lanthanide ion

Table 1
Apparent dissociation constants (K_d) for Sp1(P1)GLI and Sp1(P1G)GLI bindings to GCGLI-3 and GCGLI-10

Binding site[b]	K_d (nM)[a]	
	Sp1(P1)GLI	Sp1(P1G)GLI
GCGLI-3	$2.6(\pm0.4)\times10^2$	$2.8(\pm0.5)\times10^2$

[a] Apparent dissociation constants were determined by titration using gel mobility shift assays as described in Materials and methods. Values are averages of three or more independent determinations with standard deviations.
[b] The nomenclature is described in the text (see Fig. 1).

[16,17], we compared the DNA-binding ability in the absence or presence of 5 μM La^{3+}. As a result, a change in the DNA-binding affinity was not observed under our experimental conditions (data not shown). In consideration of these results, our designed zinc fingers seem to have the expected DNA-binding affinity for GCGLI-3 in the presence of a lanthanide ion.

Evaluation of site-specific DNA cleavage of zinc finger-type nucleases

Several lanthanide ions show effective catalytic activity for the hydrolytic cleavage of phosphate ester bonds. In particular, Ce(IV)-complexes are known to exhibit high cleavage ability [7–12]. Indeed, Ce(IV) was chelated with P1, Sp1(P1)GLI, and Sp1(P1G)GLI. Fig. 4 shows the results of the DNA cleavage experiment. First, we examined the DNA cleavage ability of the Ce(IV)–P1 complex, but no enhanced DNA cleavage pattern was detected even after a 24-h reaction. On the other hand, Sp1(P1)GLI and Sp1(P1G)GLI bound to Ce(IV) showed a clear DNA cleavage pattern inside their DNA-binding sites, depending on the concentration of proteins. Especially, the base site between two DNA-binding sites of the zinc finger domains was strongly

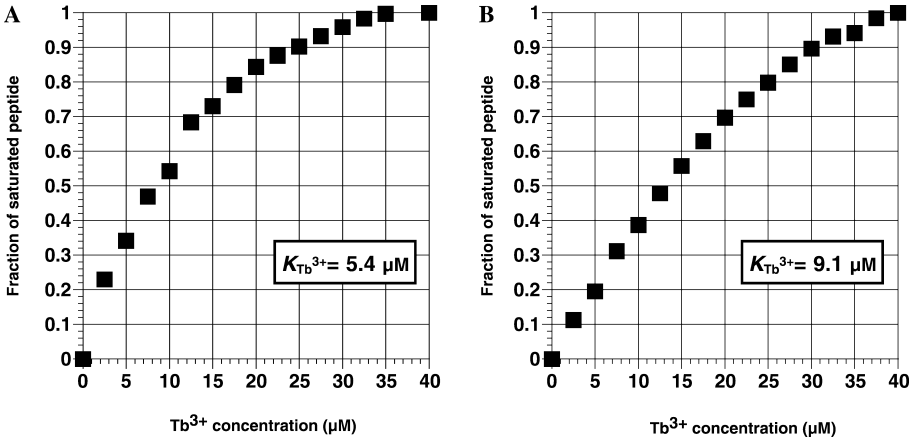

Fig. 3. (A,B) Represent the Tb^{3+} luminescence of Sp1(P1)GLI and Sp1(P1G)GLI, respectively. The fraction of peptide molecules saturated with Tb^{3+} (I/I_{max}) was calculated at a peptide concentration of 30 μM as described in Materials and methods. Excitation and emission wavelengths are 280 and 542 nm, respectively.

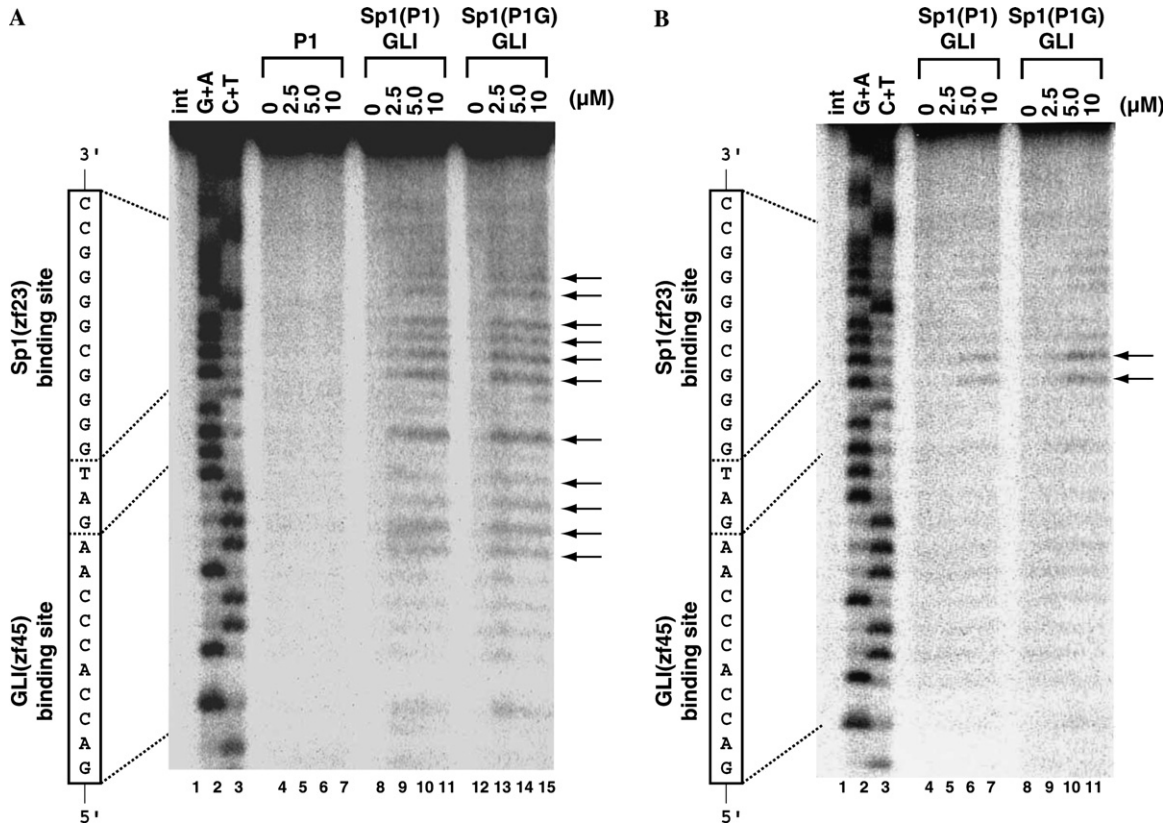

Fig. 4. Polyacrylamide gel electrophoresis for detecting the DNA cleavage of GCGLI-3. (A,B) The results of 24- and 2-h reactions, respectively. The arrow represents the enhanced sites of cleavage by adding the peptide. Lane 1, intact DNA; lane 2, G + A (Maxam–Gilbert reaction products); and lane 3, C + T (Maxam–Gilbert reaction products). Peptide concentration is noted in the figure.

cleaved. We further examined the DNA cleavage pattern in a shorter reaction time. Surprisingly, only the base site between two DNA-binding sites was specifically cleaved at 2 h, although the extent of DNA cleavage was smaller than that at 24 h. Based on the fact that the Ce–P1 complex itself has no DNA cleavage activity, the strong DNA-binding affinity of zinc finger proteins seems to cooperatively induce DNA cleavage activity of the Ce–P1 region. Of special interest is the fact that Sp1(P1G)GLI cleaved DNA more strongly than did Sp1(P1)GLI, in spite of their similar lanthanide ion and DNA-binding affinities. Presumably, the glycine-spacer in the former peptide helps the Ce(IV)–P1 region to access the substrate DNA effectively.

In contrast to previous protein-based approaches [1–10], our designed nucleases have high potential for application to any DNA sequences based on the following features: (i) the usefulness of zinc finger domains for almost all of the DNA triplets [26–31], and (ii) the facilitated engineering of multi-zinc finger-type nucleases by converting any normal linkers into P1 linkers. From our result in which Sp1(P1G)GLI showed stronger DNA cleavage activity than did Sp1(P1)GLI, a more effective nuclease would be produced by optimization of the spacer region between the DNA cleavage domain and the DNA-binding domain. Consequently, such novel zinc finger-type nucleases would provide important information for the creation of valuable artificial nucleases and for zinc finger-based design.

References

[1] R.H. Ebright, Y.W. Ebright, P.S. Pendergrast, A. Gunasekera, Conversion of a helix–turn–helix motif sequence-specific DNA binding protein into a site-specific DNA cleavage agent, Proc. Natl. Acad. Sci. USA 87 (1990) 2882–2886.

[2] Y.W. Ebright, Y. Chen, P.S. Pendergrast, R.H. Ebright, Incorporation of an EDTA-metal complex at a rationally selected site within a protein: application to EDTA-iron DNA affinity cleaving with catabolite gene activator protein (CAP) and Cro, Biochemistry 31 (1992) 10664–10670.

[3] M.G. Oakley, M. Mrksich, P.B. Dervan, Evidence that a minor groove-binding peptide and a major groove-binding protein can simultaneously occupy a common site on DNA, Biochemistry 31 (1992) 10969–10975.

[4] M. Nagaoka, M. Hagihara, J. Kuwahara, Y. Sugiura, A novel zinc finger-based DNA cutter: biosynthetic design and highly selective DNA cleavage, J. Am. Chem. Soc. 116 (1994) 4085–4086.

[5] Y.-G. Kim, J. Cha, S. Chandrasegaran, Hybrid restriction enzymes: zinc finger fusions to Fok I cleavage domain, Proc. Natl. Acad. Sci. USA 93 (1996) 1156–1160.

[6] J. Smith, M. Bibikova, F.G. Whitby, A.R. Reddy, S. Chandrasegaran, D. Carroll, Requirements for double-strand cleavage by chimeric restriction enzymes with zinc finger DNA-recognition domains, Nucleic Acids Res. 28 (2000) 3361–3369.

[7] S.J. Franklin, Lanthanide-mediated DNA hydrolysis, Curr. Opin. Chem. Biol. 5 (2001) 201–208.
[8] J.T. Welch, W.R. Kearney, S.J. Franklin, Lanthanide-binding helix-turn-helix peptides: solution structure of a designed metallonuclease, Proc. Natl. Acad. Sci. USA 100 (2003) 3725–3730.
[9] R.T. Kovacic, J.T. Welch, S.J. Franklin, Sequence-selective DNA cleavage by a chimeric metallopeptide, J. Am. Chem. Soc. 125 (2003) 6656–6662.
[10] F.H. Zelder, A.A. Mokhir, R. Kramer, Sequence selective hydrolysis of linear DNA using conjugates of Zr(IV) complexes and peptide nucleic acids, Inorg. Chem. 42 (2003) 8618–8620.
[11] W. Chen, Y. Kitamura, J.-M. Zhou, J. Sumaoka, M. Komiyama, Site-selective DNA hydrolysis by combining Ce(IV)/EDTA with monophosphate-bearing oligonucleotides and enzymatic ligation of the scission fragments, J. Am. Chem. Soc. 126 (2004) 10285–10291.
[12] Y. Yamamoto, A. Uehara, T. Tomita, M. Komiyama, Site-selective and hydrolytic two-strand scission of double-stranded DNA using Ce(IV)/EDTA and pseudo-complementary PNA, Nucleic Acids Res. 32 (2004) e153.
[13] N.P. Pavletich, C.O. Pabo, Zinc finger-DNA recognition: crystal structure of a Zif268-DNA complex at 2.1 Å, Science 252 (1991) 809–817.
[14] M. Elrod-Erickson, M.A. Rould, L. Nekludova, C.O. Pabo, Zif268 protein–DNA complex refined at 1.6 Å: a model system for understanding zinc finger–DNA interactions, Structure 4 (1996) 1171–1180.
[15] S.A. Wolfe, L. Nekludova, C.O. Pabo, DNA recognition by Cys2His2 zinc finger proteins, Annu. Rev. Biophys. Biomol. Struct. 29 (2000) 183–212.
[16] J. Wojcik, J. Goral, K. Pawlowski, A. Bierzynski, Isolated calcium-binding loops of EF-hand proteins can dimerize to form a native-like structure, Biochemistry 36 (1997) 680–687.
[17] M. Siedlecka, G. Goch, A. Ejchart, H. Sticht, A. Bierzynski, α-Helix nucleation by a calcium-binding peptide loop, Proc. Natl. Acad. Sci. USA 96 (1999) 903–908.
[18] M.M. Lopez, D.-H. Chin, R.L. Baldwin, G.I. Makhatadze, The enthalpy of the alanine peptide helix measured by isothermal titration calorimetry using metal-binding to induce helix formation, Proc. Natl. Acad. Sci. USA 99 (2002) 1298–1302.
[19] D.-H. Chin, R.W. Woody, C.A. Rohl, R.L. Baldwin, Circular dichroism spectra of short, fixed-nucleus alanine helices, Proc. Natl. Acad. Sci. USA 99 (2002) 15416–15421.
[20] N.P. Pavletich, C.O. Pabo, Crystal structure of a five-finger GLI-DNA complex: new perspectives on zinc fingers, Science 261 (1993) 1701–1707.
[21] M. Yokono, N. Saegusa, K. Matsushita, Y. Sugiura, Unique DNA binding mode of the N-terminal zinc finger of transcription factor Sp1, Biochemistry 37 (1998) 6824–6832.
[22] Y. Shiraishi, M. Imanishi, Y. Sugiura, Exchange of histidine spacing between Sp1 and GLI zinc fingers: distinct effect of histidine spacing-linker region on DNA binding, Biochemistry 43 (2004) 6352–6359.
[23] S. Oka, Y. Shiraishi, T. Yoshida, T. Ohkubo, Y. Sugiura, Y. Kobayashi, NMR structure of transcription factor Sp1 DNA binding domain, Biochemistry 43 (2004) 16027–16035.
[24] J.L. Vazquez-Ibar, A.B. Weinglass, H.R. Koback, Engineering a terbium-binding site into an integral membrane protein for luminescence energy transfer, Proc. Natl. Acad. Sci. USA 99 (2002) 3487–3492.
[25] M. Dadlez, J. Goral, A. Bierzynski, Luminescence of peptide-bound terbium ions: determination of binding constants, FEBS Lett. 282 (1991) 143–146.
[26] Y. Choo, A. Klug, Toward a code for the interactions of zinc fingers with DNA: selection of randomized fingers displayed on phage, Proc. Natl. Acad. Sci. USA 91 (1994) 11163–11167.
[27] Y. Choo, A. Klug, Selection of DNA binding sites for zinc fingers using rationally randomized DNA reveals coded interactions, Proc. Natl. Acad. Sci. USA 91 (1994) 11168–11172.
[28] H.A. Greisman, C.O. Pabo, A general strategy for selecting high-affinity zinc finger proteins for diverse DNA target sites, Science 275 (1997) 657–661.
[29] D.J. Segal, B. Dreier, R.R. Beerli, C.F. Barbas III, Toward controlling gene expression at will: selection and design of zinc finger domains recognizing each of the 5′-GNN-3′ DNA target sequences, Proc. Natl. Acad. Sci. USA 96 (1999) 2758–2763.
[30] B. Dreier, R.R. Beerli, D.J. Segal, J.D. Flippin, C.F. Barbas III, Development of zinc finger domains for recognition of the 5′-ANN-3′ family of DNA sequences and their use in the construction of artificial transcription factors, J. Biol. Chem. 276 (2001) 29466–29478.
[31] T. Sera, C. Uranga, Rational design of artificial zinc-finger proteins using a nondegenerate recognition code table, Biochemistry 41 (2002) 7074–7081.